Macromolecules
ARTICLE

Linear Free-Energy Relationships for the Alkyl Radical Affinities of Nitroxides: A Theoretical Study

Jennifer L. Hodgson, Ching Yeh Lin, and Michelle L. Coote*

ARC Center of Excellence for Free-Radical Chemistry and Biotechnology, Research School of Chemistry, Australian National University, Canberra ACT 0200, Australia

Sylvain R. A. Marque*

UMR 6264 Laboratoire Chimie Provence, case 521, Universite de Provence, Avenue Escadrille Normandie Niemen, 13397 Marseille Cedex 20, France

Krzysztof Matyjaszewski*

Department of Chemistry, Carnegie Mellon University, 4400 Fifth Avenue, Pittsburgh, Pennsylvania 15213

ABSTRACT: High-level *ab initio* calculations have been used to construct linear free-energy relationships describing the kinetics and thermodynamics of the combination and dissociation reactions between alkyl radicals and nitroxides in terms of easily accessible parameters that quantify the electronic, steric and radical stabilization characteristics of the coreactants. For the gas-phase equilibrium constant ($K_{eq} = k_c/k_d$) of the combination reaction at 298 K, the following equation was obtained: $\log (K_{eq}) = -0.10\text{IP} - 0.177\text{RSE} - 0.130\text{RSE}_{nxd} + 38.3$. In this equation, IP is the vertical ionization potential of the alkyl radical, RSE is the standard radical stabilization energy the alkyl radical, while RSE_{nxd} is a new descriptor for the nitroxide radical, related to the standard radical stabilization energy, but measuring in this case the flexibility of the nitroxide to the geometric changes associated with formation of an alkoxyamine. The equation was successful for combinations of substituents not included in the original fitting and can thus be used to predict the behavior for larger systems for which direct calculation is impractical. Similar equations were also fitted to available experimental data for k_c, at 298 K and k_d, at 393 K, both in *tert*-butyl benzene, to allow the prediction of rate constants. The equation-determined rate constants, $k_{c,eq}$ and $k_{d,eq}$ are given by $\log (k_{c,eq}) = -0.408\text{IP} - 0.0597\text{RSE} - 0.103\text{RSE}_{nxd} + 14.5$ and $\log (k_{d,eq}) = 0.794\text{IP} + 5.68\theta + 0.0873\text{RSE} + 0.0821\text{RSE}_{nxd} - 27.7$. For the decomposition rate, an additional parameter, Tolman's cone angle θ, which measures the steric bulk of the attacking alkyl radical, was found to improve the fit to the data. The equations could in principle be fitted to experimental or calculated rate and equilibrium constants under a variety of reaction conditions. On the basis of our analysis, it appears that the stability of the alkyl radical has the largest effect on the kinetics and thermodynamics of the combination and dissociation reactions, with smaller but significant contributions from the remaining parameters.

1. Introduction

Quantitative relationships between the structure, properties and reactivities of molecules are well-known, and linear free-energy relationships comprising quantitative steric and electronic descriptors have been used to predict the kinetic and thermodynamic properties of many types of organic,[1,2] inorganic,[3-5] and biological[6] reactions. Typically these relationships take the form

$$\text{property} = aE + bS + c \qquad (1)$$

where *a*, *b*, and *c* are constants and *E* and *S* are quantitative measurements of electronic and steric effects, respectively. For reactions involving radicals, the stabilization energies of these species are also expected to play a role.

Recently, linear free energy relationships have been investigated in the design of optimal control agents for nitroxide-mediated polymerization (NMP).[7-9] Since its discovery, NMP[10-12] along with the other controlled radical polymerization process such as ATRP[13] and RAFT,[14] has become a widely used technique for controlling the molecular weight and architecture of the polymer produced in free radical polymerization. These methods have become increasingly popular due to their simplicity and robustness combined with their ability to create designer architectures for use in nanotechnology and biotechnology applications. Control is achieved through the reversible combination of the growing alkyl polymeric radical by a nitroxide radical species so as to form a dormant alkoxyamine (eq 2)

$$\text{RR'NO}^{\bullet} + \text{P}_n^{\bullet} \underset{k_d}{\overset{k_c}{\rightleftharpoons}} \text{RR'NO–P}_n \qquad (2)$$
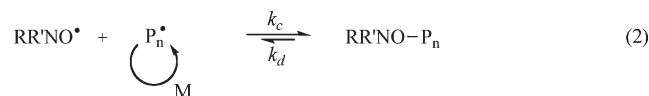
The rate constants of combination and dissociation, k_c and k_d, and their relationship described by $K = k_c/k_d$, are important parameters in determining the success of the control reaction and hence the properties of the polymer produced.[15-17] If K is too

*Correspondence authors. E-mail: (M.L.C.) mcoote@rsc.anu.edu. au; (S.R.A.M.) sylvain.marque@univ-provence.fr; (K.M.) km3b@ andrew.cmu.edu.

small, especially in the case that k_c is small, not enough of the growing polymer will be trapped at any one time to afford control, resulting in polymers with high molecular mass dispersity (i.e., high M_w/M_n values). On the other hand, if K is too large, too much of the growing polymer will remain trapped in a dormant form and the polymerization will occur sluggishly, also resulting in poor control. Kinetic analyses by Souaille and Fischer for generic living polymerizations controlled by a reversible combination reaction showed that, for efficient control, the equilibrium constant, K, should vary roughly from 10^7 to 10^{11} L mol^{-1}.[18,19] It should also be noted that the success of NMP depends on additional factors including the dynamics of the exchange between the active and dormant species, as well as the stability of the nitroxide and alkoxyamine toward side reactions, such as the formation the corresponding hydroxylamine and alkene species via hydrogen transfer, which occurs in the case of methacrylate polymerization.[20] Provided these additional factors are also taken into account, it is clear that an understanding of the effects of the chemical structure of the propagating radical and nitroxide on the equilibrium constants can greatly assist in the selection and design of improved control agents for this process.

Several investigators have observed that the forward and reverse rates of the control reaction are affected by the structure of the nitroxide radical, including its ring size, steric bulk, potential for intramolecular hydrogen bonding, and the polar effects from groups attached to the ring.[21−24] These effects have been quantified using parameters such as bond dissociation energies, radical stabilization, polar, and steric factors.[25] Equations to predict combination and dissociation rate constants for the reaction between various nitroxide radicals with the styrene unimeric radical have been determined.[7,9] In these equations k_c and k_d are expressed in terms of the Hammett parameter for polar/inductive field (σ_I)[26] and the Taft parameter for steric effects (E_s),[27−29] for substituents on the nitroxide.

Separately, the stability, polarity and steric bulk of the leaving alkyl radical were found to affect the rate of the dissociation reaction in a similar way.[8,21] Equations describing the dissociation rate constants for various 2,2,6,6,-tetramethylpiperidin-1-yloxyl (TEMPO) and *N-tert*-butyl-*N*-[1-diethylphosphono-2,2-dimethylpropy)] nitroxide (SG1) type alkoxyamines have been determined.[8] In these equations, the dissociation rate constant has been expressed in terms of the Charton parameters for polar/inductive field (σ_U)[26] and steric effects (v),[30] as well as a parameter quantifying the radical stability (σ_{RS}), as determined by Rüchardt et al.[31,32]

Although successful, the equations determined previously to describe the combination and dissociation reactions of nitroxides and alkyl radicals are not general. They describe the rate constants of the reactions for the variation of either the nitroxide radical or the alkyl radical separately, but are not applicable for the variation of both simultaneously. They also use various experimentally determined parameters, and in many cases these are not available in the literature and must be instead estimated by additivity approximations.[26,32−34] These approximations do not account for the influence of penultimate units and other remote substituents; however, there is growing evidence that these effects are significant in nitroxide mediated polymerization,[35,36] and indeed in other conventional[37] and controlled radical polymerization processes.[38,39]

To address these problems, in the present work, we design and test a new equation to describe the thermodynamics and kinetics of nitroxide combination reactions in terms of easily accessible parameters representing polar, steric and radical stability factors, and generalized for all combinations of nitroxide controlling agents and monomers. To this end, we examine and assess the suitability of the various alternative parameters that have been proposed in the literature for describing these properties of the propagating radical, before repeating the assessment process for the nitroxide radicals. Our primary criteria for selecting our final computational descriptors are that they are chemically intuitive, reasonably well correlated with the well-known empirical parameters utilized in the original equation, and easily accessible, even for larger and/or unusual species. Using our selected parameters, we then design, fit, and test our new equation against rate and equilibrium constants for a variety of propagating radical and nitroxide combinations.

2. Theoretical Methods

Standard *ab initio* molecular orbital[40] and density functional[41] calculations in this work were carried out using GAUSSIAN 03[42] and MOLPRO 2000.6.[43] It should be noted that all radicals and all closed-shell species considered in this study were true (local) minimum energy structures (i.e., having no imaginary frequencies). Determination of correlation coefficients, best-fit parameters and associated test statistics for our various equations were performed using standard linear regression techniques integrated into Microsoft Excel.

Geometries of all species were optimized at the B3-LYP/ 6-31G(d) level of theory, with conformations systematically screened to ensure that species were global minimum energy structures. Frequency calculations were performed at the same level and scaled via the appropriate factors.[44] Mulliken spin densities and dipole moments are both based on optimized geometries at the B3-LYP/6-31G(d) level of theory. The thermodynamics of combination reactions as well as other reaction based descriptors such as gas-phase vertical ionization potentials (IP) and radical stabilization energies (RSE) were then obtained at the G3(MP2)-RAD[45] level of theory. This high-level *ab initio* molecular orbital theory method is designed to reproduce CCSD(T) calculations with a large triple-ζ basis set via additivity approximations. It has been shown to reproduce a large test set of experimental gas-phase thermochemical data to within a mean absolute deviation (MAD) of 5.17 kJ mol^{-1}.[45] Gas-phase electron affinities (EA) were calculated using a variant of G3(MP2)-RAD in which calculations with the 6-31G(d) basis set were replaced with corresponding calculations with the 6-31+G(d) basis set, so as to allow for better treatment of anionic species. For larger species, we made use of an ONIOM approximation in which the core of the reaction (chosen to include full polymeric radical while truncating the nitroxyl fragment at the β substituents) was studied at G3(MP2)-RAD and the remaining substituent effects of the full system were studied at the RMP2/ 6-311+G(3df,2p) level of theory. We have previously demonstrated that this approach approximates full G3(MP2)-RAD calculations to within chemical accuracy for a large test set of radical reactions including those directly relevant to the present work.[46]

As part of this work, we carry out a small assessment study in which we compare our calculated equilibrium constants with available experimental data. In order to make direct comparisons, equilibrium constants of the various combination reactions were calculated at the same temperatures and in the same solvent medium. Solution phase free energies were obtained by a thermodynamic cycle in which gas-phase energies were obtained using high-level *ab initio* methods as described above and then added to free energies of solvation, as calculated using the polarized continuum model PCM[47] at the B3-LYP/6-31G(d) level. The PCM calculation was carried out using the united atom topological model with the recommended optimization of radii (i.e., the UAKS keyword in the GAUSSIAN calculation). These methods have previously shown success in the calculation of solution phase equilibrium constants of the control reactions of ATRP[48,49]

Scheme 1. Nitroxide and Alkyl Radicals
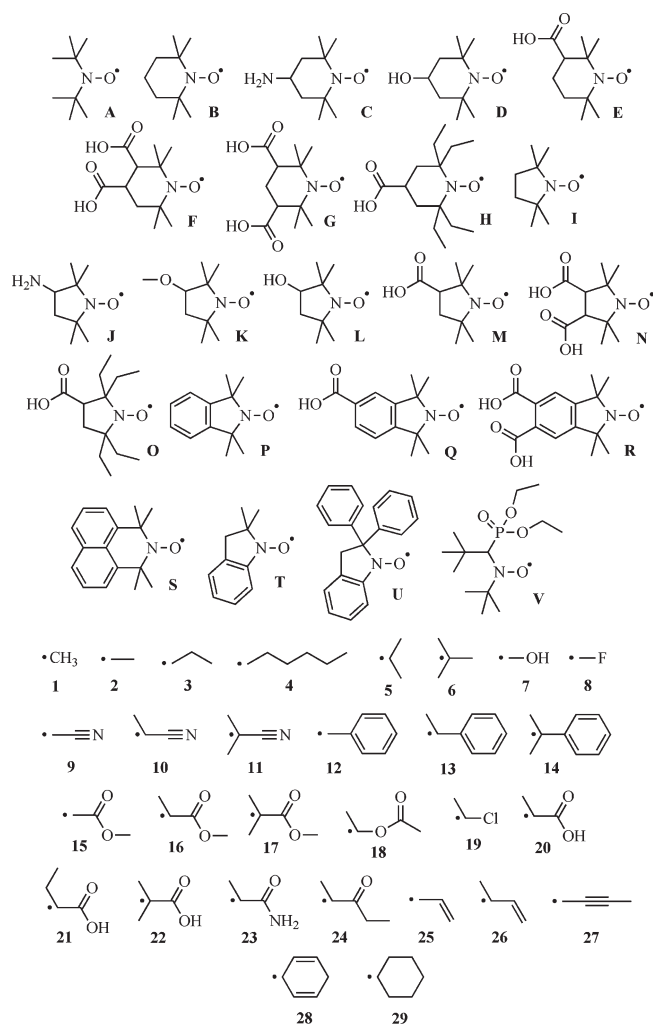
and RAFT[50] and in determinations of the one-election oxidation and reduction potentials of nitroxide radicals in both water and acetonitrile.[51,52]

To study the steric properties of alkyl radicals, the molecular volume (V), anchor volume (V^a), and cone volume (CV), Tolman's cone angle (θ), and solid angle (Ω) of these species were also calculated on the B3-LYP/6-31G(d) optimized geometries of the TEMPO alkoxyamines, using the Bondi's van der Waals radii[53] and Cambridge Structural Database (CSD) covalent radii.[54] The anchor volume is defined as the volume within a 0.3 Å radius around the anchor atom.[55] The solid angle was calculated using the program "Steric", which is available for download.[56]

3. Results

Nitroxide and alkyl radical species included in this study are shown in Scheme 1. Specifically, we define two *training sets*, which are used to parametrize our equation, and a *test set*, which is used to test its predictive capabilities. Training set I comprises combination reactions of 2,2,6,6-tetramethyl-piperidin-1-yloxyl (TEMPO, **B**) with a broad range of alkyl radicals, including ethyl (**2**), propyl (**3**), isopropyl (**5**) and *tert*-butyl (**6**) radicals, •CH₂OH (**7**), •CH₂F (**8**), •CH₂CN (**9**), •CH(CH₃)CN (**10**), •C(CH₃)₂CN (**11**), •CH₂Ph (**12**), •CH(CH₃)Ph (**13**), •C(CH₃)₂Ph (**14**), •CH₂COOCH₃ (**15**), •CH(CH₃)COOCH₃ (**16**), •C(CH₃)₂COOCH₃, (**17**) •CH(CH₃)OC(O)CH₃ (**18**), and •CH(CH₃)Cl (**19**). These were chosen to include common polymeric unimers, as well as

several additional species chosen to cover a broad range of electronic and steric properties. Training set II includes combination reactions of the methyl radical with 6-membered cyclic derivatives of TEMPO (**B**), 1,1,3,3-tetramethyl-2,3-dihydro-2-azaphenalene-2-yloxyl (TMAO, **S**), 5-membered cyclic derivatives of 2,2,5,5-tetramethyl-pyrrolidin-1-yloxyl (PROXYL, **I**), 2,2-dimethylindolin-1-yloxyl (**T**), 1,1,3,3-tetramethylisoindolin-2-yloxyl (TMIO, **P**), and the acyclic species ditert-butyl nitroxide (DBN, **A**) and *N-tert*-butyl-*N*-[1-diethylphosphono-2,2-dimethyl-propy)] nitroxide (SG1, **V**). Our test set comprises various combinations of these alkyl radicals and nitroxides not included in the training sets and is designed to be representative of more practical polymerization systems. These include combinations of unimers for styrene (•CH(CH₃)Ph (**13**)), acrylic acid (•CH(CH₃)COOH (**20**)) methyl acrylate (•CH(CH₃)COOCH₃ (**16**)), methyl methacrylate (•CH(CH₃)COOCH₃ (**17**)), and acrylamide (•CH(CH₃)CONH₂ (**23**)) with DBN (**A**), TEMPO (**B**), PROXYL (**I**), and TMIO (**P**). The 298 K gas-phase equilibrium constants for combination reactions of these species were obtained in the present work using high-level *ab initio* molecular orbital theory calculations and are shown in Table 1, along with values of their relevant polar, steric and radical stabilization descriptors; details of these parameters are provided in the next section. Complete optimized geometries are provided in Appendix S1 of the Supporting Information.

4. Discussion

In what follows we examine the physical basis of a wide variety of computed electronic (μ, EA, IP and ω), steric ($-E$'s, E_R, V, V^a, CV, order, θ, and Ω) and radical stabilization parameters (RSE, ρ, and $\rho\%$), and compare them with the empirical alkyl radical descriptors σ_U, v, and σ_{RS} used in the original[8] linear free energy relationship for combination reactions of alkyl radicals and nitroxides. On this basis, we then select suitable parameters for modeling the effect of the alkyl radical on combination reactions with a specified nitroxide. We then design a new nitroxide radical parameter RSE$_{nxd}$, which quantifies the effect of the nitroxide radical on combination reactions with a fixed alkyl radical. Finally, the computed parameters are combined into general equations to describe the thermodynamics and kinetics of the combination reaction for any combination of alkyl radical and nitroxide. Before proceeding to this analysis, we first evaluate the accuracy of our computational chemistry calculations against available experimental data.

Assessment of Computational Methods. Computational chemistry has previously been used to study structure−reactivity trends in the bond dissociation energies of alkoxy-amines.[57,58] The density functional theory methods used were able to reproduce the qualitative trends when compared to experimental data, but showed some systematic errors. In this work, we utilize a high-level methodology that has been both quantitatively and qualitatively successful in predicting the redox potentials of nitroxides in aqueous and nonaqueous solution,[51,52] as well as the kinetics[59,60] and thermodynamics[48−50,61] of a wide range of radical reactions in solution including those directly relevant to conventional and controlled radical polymerization processes.[62] In this section, we carry out further testing of our methodology through direct comparison of our calculated equilibrium constants for nitroxide combination reactions with corresponding experimental values, as obtained from measured rate coefficients.

Calculated solution-phase equilibrium constants for radical combination reactions of various carbon-centered radicals with nitroxides are shown in Table 2, along with available experimental data. The experimental equilibrium

Table 1. Calculated log (K_{calc}) Values (298 K)[a] and Descriptors for Combination Reactions of Alkyl Radicals with Nitroxides Making up the Training and Test Sets

species	log (K_{calc})	alkyl descriptors					nitroxide descriptor
		μ (D)	IP (eV)[c]	θ (deg)	ρ[d]	RSE (kJ mol^{-1})	RSE$_{nxd}$ (kJ mol^{-1})
				Training Set I			
B1	28.0	0.00	9.88	1.85	1.16	0.0	−4.3
B2	28.6	0.25	8.63	2.05	1.09	14.1	−4.3
B3	29.2	0.23	8.49	2.04	1.09	12.6	−4.3
B5	27.0	0.20	7.80	2.26	1.02	24.0	−4.3
B6	24.6	0.19	7.22	2.47	0.96	29.7	−4.3
B7	30.9	1.55	8.21	1.98	0.93	31.5	−4.3
B8	34.7	1.25	9.61	1.98	0.99	12.4	−4.3
B9	22.4	3.35	10.31	2.04	0.89	31.9	−4.3
B10	21.6	3.89	9.36	2.25	0.84	47.3	−4.3
B11	17.7[b]	4.13	8.64	2.46	0.80	59.0	−4.3
B12	20.7[b]	0.13	7.39	2.06	0.79	59.0	−4.3
B13	19.8[b]	0.38	7.03	2.37	0.77	68.0	−4.3
B14	17.6[b]	0.65	6.73	2.67	0.75	69.9	−4.3
B15	24.0	1.75	9.91	2.13	0.97	21.5	−4.3
B16	22.1[b]	1.65	8.92	2.34	0.89	41.2	−4.3
B17	18.9[b]	1.97	8.27	2.58	0.83	54.9	−4.3
B18	31.1[b]	1.85	7.65	2.11	0.98	24.4	−4.3
B19	28.7	1.65	8.27	2.26	0.96	27.0	−4.3
				Training Set II			
A1	26.7	0.00	9.88	1.85	1.16	0.0	0.0
C1	28.5	0.00	9.88	1.85	1.16	0.0	−5.6
D1	28.3	0.00	9.88	1.85	1.16	0.0	−6.5
E1	28.6	0.00	9.88	1.85	1.16	0.0	−8.2
F1	28.9[b]	0.00	9.88	1.85	1.16	0.0	−10.4
G1	29.5[b]	0.00	9.88	1.85	1.16	0.0	−13.3
H1	25.6[b]	0.00	9.88	1.85	1.16	0.0	3.3
I1	25.8	0.00	9.88	1.85	1.16	0.0	9.9
J1	26.3	0.00	9.88	1.85	1.16	0.0	7.8
K1	26.9	0.00	9.88	1.85	1.16	0.0	5.0
L1	26.8	0.00	9.88	1.85	1.16	0.0	7.7
M1	26.2	0.00	9.88	1.85	1.16	0.0	6.9
N1	26.7[b]	0.00	9.88	1.85	1.16	0.0	3.8
O1	24.5[b]	0.00	9.88	1.85	1.16	0.0	15.6
P1	26.3	0.00	9.88	1.85	1.16	0.0	7.2
Q1	26.5[b]	0.00	9.88	1.85	1.16	0.0	4.9
R1	26.9[b]	0.00	9.88	1.85	1.16	0.0	2.4
S1	28.3	0.00	9.88	1.85	1.16	0.0	−3.3
T1	27.6	0.00	9.88	1.85	1.16	0.0	0.3
U1	28.8[b]	0.00	9.88	1.85	1.16	0.0	−11.4
V1	25.9[b]	0.00	9.88	1.85	1.16	0.0	5.8
				Test Set			
A13	17.2[b]	0.38	7.03	2.37	0.77	68.0	0.0
A16	20.2[b]	1.65	8.92	2.34	0.89	41.2	0.0
A17	17.2[b]	1.97	8.27	2.58	0.83	54.9	0.0
A20	19.5[b]	1.64	8.50	2.29	0.89	41.2	0.0
A23	21.7[b]	3.49	8.79	2.60	0.91	41.0	0.0
B20	21.5[b]	1.64	8.50	2.29	0.89	41.2	−4.3
B23	24.3[b]	3.49	8.79	2.60	0.91	41.0	−4.3
I13	18.3[b]	0.38	7.03	2.37	0.77	68.0	9.9
I16	20.8[b]	1.65	8.92	2.34	0.89	41.2	9.9
I17	17.5[b]	1.97	8.27	2.58	0.83	54.9	9.9
I20	20.4[b]	1.64	8.50	2.29	0.89	41.2	9.9
I23	22.5[b]	3.49	8.79	2.60	0.91	41.0	9.9
P13	18.9[b]	0.38	7.03	2.37	0.77	68.0	7.2
P16	20.8[b]	1.65	8.92	2.34	0.89	41.2	7.2
P17	18.3[b]	1.97	8.27	2.58	0.83	54.9	7.2
P20	20.4[b]	1.64	8.50	2.29	0.89	41.2	7.2
P23	22.6[b]	3.49	8.79	2.60	0.91	41.0	7.2

[a] G3(MP2)-RAD//B3-LYP/6-31G(d) values except where noted. [b] ONIOM approximation with the full system calculated at the RMP2/6-311+G(3df,2p) level. [c] Vertical ionization potential. [d] Spin density on the radical center.

constant, $K = k_c/k_d$, was obtained by combining independently measured values of the rate coefficients for the forward, k_c, and reverse, k_d, combination reactions. Since the experimental measurements were performed at 393 K in *tert*-butyl benzene (*t*BB), the *ab initio* equilibrium constants were also calculated at 393 K from the solution-phase reaction free energies of the individual species determined in the closely related solvent toluene. Figure 1 compares the calculated equilibrium constants of the combination of alkyl radicals with nitroxides, and the experimentally determined

Table 2. Calculated and Experimental Equilibrium Constant for Nitroxide Combination Reactions Measured at 393 K in *tert*-Butyl Benzene Except Where Noted[a]

Nitroxide	Radical		$k_{c,393,tBB}$ (Lmol^{-1}s^{-1})	$k_{d,393,tBB}$ (s^{-1})	Experimental $K_{393} = k_c/k_d$	Calculated $K_{393,toluene}$ (Lmol^{-1})[i]
	·	A12	2.1×10^{8} [a]	1.9×10^{-4} [e]	1.1×10^{12}	4.1×10^{11}
	·	B12	3.5×10^{8} [a]	1.1×10^{-5} [e]	3.2×10^{13}	7.8×10^{12}
		B13	2.5×10^{8} [a]	5.2×10^{-4} [e]	4.8×10^{11}	2.6×10^{11}
		B14	5.5×10^{7} [a]	8.5×10^{-2} [e]	6.5×10^{8}	4.5×10^{9}
		B15	2.3×10^{9} [a,b,c]	8.1×10^{-8} [e,f]	2.8×10^{16}	4.8×10^{15}
		B17	5.9×10^{8} [a,b]	2.2×10^{-2} [e,g]	2.7×10^{10}	4.7×10^{10}
		P13	1.5×10^{8} [d]	2.2×10^{-4} [e,h]	6.8×10^{11}	2.3×10^{10}
		P14	1.5×10^{8} [a]	4.1×10^{-2} [e,h]	3.7×10^{9}	3.0×10^{9}

[a] Values at 393 K were obtained by extrapolation from data points measured at 297 and 323 K.[63] [b] Measured in acetonitrile. [c] Measured at 297 K. [d] Measured at 293 K.[7] [e] Measured at 393 K.[21] [f] For reaction with a ·CH$_2$COOt-Bu radical. [g] For reaction with a ·C(CH$_3$)$_2$COOt-Bu radical. [h] Calculated from estimated activation energies.[21] [i] ONIOM approximation of G3(MP2)-RAD//B3-LYP/6-31G(d) values including (CH$_3$)$_2$NO· and the alkyl radical in the core system, with the full system calculated at the RMP2/6-311+G(3df,2p) level. Free energy of solvation calculated using PCM at the B3-LYP/6-31G(d) level using the united atom topological model with the recommended optimization of radii (UAKS keyword in GAUSSIAN).
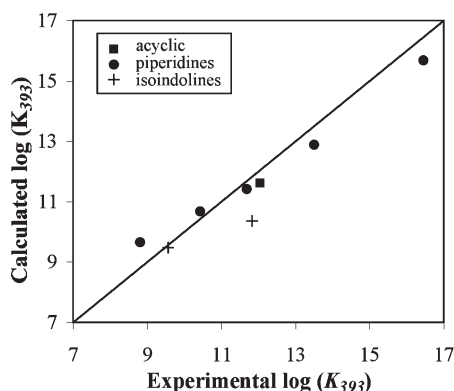
Figure 1. Comparison of experimental and calculated equilibrium constants for combination reactions of nitroxides with alkyl radicals (MAD = 4.5 kJ mol^{-1}).

values. The mean absolute deviation in the data corresponds to a difference in free energy of 4.5 kJ mol^{-1}, which is excellent considering the likely level of uncertainty in the experimental data itself. The maximum deviation is observed for the combination of the phenyl ethyl radical, ·CH(CH$_3$)Ph (**13**), with the five-membered isoindoline derivative TMIO (**P**). The calculated value for this reaction shows a deviation from experiment corresponding to 11.1 kJ mol^{-1} in free energy. In this particular case, the larger deviation may be due the k_c value being measured at a lower temperature than the k_d value, and the fact that an estimated activation energy was required to determine k_d.

Descriptors for the Alkyl Radicals. A wide variety of parameters have been used in the literature for quantifying the electronic, steric and radical stabilization properties of a chemical species. Table 3 lists the principal ones alongside the measure of their correlation with the corresponding empirical parameters utilized in the original equation.[8] A complete list of literature and computed parameters for the radical species studied can be found in the Supporting

Information (Tables S.1−3). We now examine the electronic, steric and stabilization parameters in turn.

Electronic Effects. The electronic (or polar) effect within a molecule describes how electrons are distributed around the substituents of interest. Electronic descriptors can be separated into a localized contribution and delocalized contribution: the localized contribution comes from a field effect through space or an inductive effect through a bond, and the delocalized contribution can be seen as a resonance effect. Electronic descriptors were first derived from fitting to pK_a values of ester hydrolysis by Hammett.[69] This model was then improved by Taft through the addition of a steric parameter to better describe the reaction rates, leading to the following polar parameter:

$$\sigma^* = \log\left(\frac{k_s}{k_{CH_3}}\right)_B - \log\left(\frac{k_s}{k_{CH_3}}\right)_A \qquad (3)$$

Here k_s is the observed rate for the acid-catalyzed ester hydrolysis, k_{CH_3} is the rate of the reference methyl, and A and B stand for the acid or base catalyzed hydrolyses of carbonyl substituted esters, respectively. Charton further refined σ^* into localized and delocalized terms, where σ_U represents the localized inductive term,[64] and unknown polar descriptors can be obtained from fitting equations.[70] Although values for a large number of species are available and equations can be used to fit many more, use of the σ_U parameter is limited by the availability of experimental data, particularly for the larger species relevant to radical polymerization processes.

There are several ways in which computationally based parameters can be used to describe electronic effect within a molecule. Although it is possible to compute the ester hydrolysis on which the σ_U term is based, this method is not computationally economical, particularly for large species. The dipole moment of the molecule, μ, is a measure of the polarity of the molecule that is computationally cheap to determine and does not rely on chemical reaction energies.

Table 3. Correlation[a] of Empirical and Computational Alkyl Radical Descriptors

property	descriptor	description	R^2
electronic	σ_U	Charton parameter for polar/inductive field[64]	1
	μ	dipole moment	0.60
	EA	electron affinity	0.58
	IP	ionization potential	0.08
	ω	global electrophilicity[65]	0.48
steric	υ	Charton steric parameter[30]	1
	E'_s	Dubois steric parameter[66]	0.66
	V	molecular volume	0.22
	V^a	anchor volume[55]	0.30
	CV	cone volume	0.09
	E_R	Ligand repulsion energy[5]	0.65
	θ	Tolman's cone angle[3]	0.77
	Ω	solid angle[56]	0.36
	order	order of radical center (primary = 1, secondary = 2, etc.)	0.79
radical stabilization	σ_{RS}	normalized values of Rüchardt RSE[8]	1
	ρ	Mulliken spin density[40]	0.91[b]
	$\rho\%$	delocalization of spin density[67]	0.78[b]
	RSE	radical stabilization energy (isodesmic reaction)[68]	0.92

[a] R^2 calculated with respect to previously used empirical descriptors.[8] [b] Show an inverse correlation.
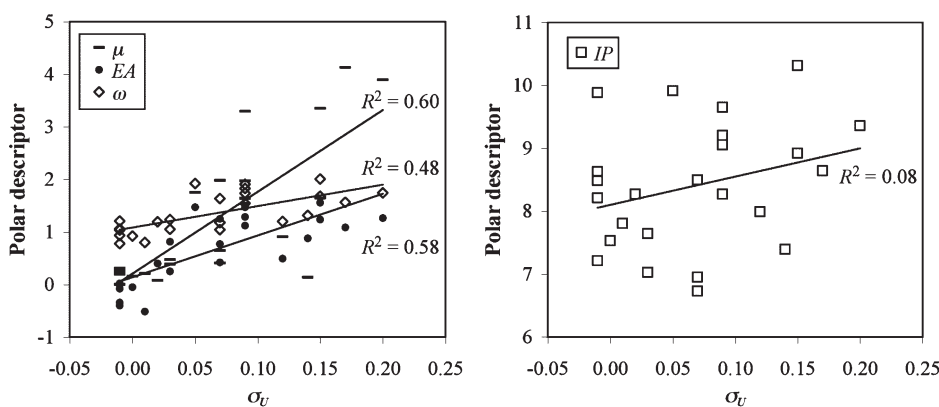

Figure 2. Comparison of the computed and empirical polar descriptors.

Alternatively, the gas-phase vertical electron affinity (EA) and ionization potential (IP) are more commonly used as electronic descriptors, and have the advantage that they are easily accessible from experiment as well as theory. The global electrophilicity, ω, as defined by Parr et al.[65] is found from the following combination of IP and EA:

$$\omega = \frac{(IP + EA)^2}{8(IP - EA)} \qquad (4)$$

Figure 2 shows the correlation between the various calculated electronic descriptors and Charton polar inductive/ field parameter σ_U; raw data are provided in Table S.1 of the Supporting Information. It is seen that the correlations between σ_U and the various computed parameters are poor. This almost certainly reflects 'deficiencies' in the original Charton parameter, as well as in the alternative computed parameters. In essence, all parameters except for the dipole moment are based ultimately on chemical reaction energies and will therefore almost certainly contain contributions from other factors, such as steric effects or, in case of IP, EA, and ω, the stability of the corresponding radical species. These additional factors are then aliased with the measured polar factors to differing extents depending upon the reaction studied. This may be an advantage when designing an equation to model reaction energies, provided the additional contributors to the polar descriptor are present to a related extent in the new reaction being modeled. In this regard the

IP is probably the most suitable of the reaction energy based descriptors for modeling the reaction energies for combination of alkyl radicals and nitroxides, despite its poor correlation with σ_μ. This is because the IP of $R^\bullet$ depends on the relative stabilities of the $R^\bullet$ and R^+, and the combination reaction energy will be influenced among other things by the relative stability of $R^\bullet$ and $R-ONR'R''$. Since the nitroxide is a good electron acceptor, its stability in turn will be affected by the potential for resonance with its ionic form, $R^{+-}ONR'R''$, and hence the stability of R^+. For this reason the IP was selected for further consideration.

Although a reaction energy based parameter may be well suited for modeling the energies of related chemical reactions, it is less suitable for studying the relative importance of polar, steric, and radical stabilization effects. For that purpose, the dipole moment provides a much more direct approach to measuring the polarity of a species, independent of contributions from the stabilities of other species. It can also be calculated accurately at a much lower level of theory, and in that sense is more readily applied to larger species, such as dimer and trimer propagating radicals. However, a disadvantage of this parameter is that it reflects the polarity of the molecule as a whole, rather than the specific ability of the alkyl group to donate or accept electrons through the attached carbon. Thus, in some cases, one could envisage the polarity of an alkyl group being high due to, for example, the presence of a highly polar remote substituent, though the alkyl group itself is a poor stabilizer of the alkoxyamine.[71,72] Despite this potential limitation, the dipole moment can

provide the most direct measure of polar effects of the parameters considered, and for this reason, it was selected for further study.

Steric Effects. The steric descriptor appears to be the most widely and diversely studied descriptor in the literature, indicating the difficulty in modeling it accurately. Steric effects were determined to be an important variable in structure versus reactivity relationships after pioneering work by Taft,[1] who systematically studied the connection between steric effects and the rate constants of reactions. It was known that polar effects were not the only influence in Hammett's equation, therefore, Taft proposed that the relative rates of esters hydrolysis should also include a steric effect.[1d] His first attempt to quantify the steric effect defined the average relative rate of acid-catalyzed ester hydrolysis as

$$E_s = \log\left(\frac{k_s}{k_{CH_3}}\right) \quad (5)$$

where k_s is the observed rate for the acid-catalyzed ester hydrolysis and k_{CH_3} is the rate using methyl as reference; these k_s are identical to those described in eq 3. Dubois standardized the measurement of conditions for ester hydrolysis and developed an improved steric descriptor, E'_s.[66] Recently, the Charton steric descriptor v was designed from van der Waals radii for MZ_n type of molecules and used to fit E'_s for asymmetrical molecules.[30]

In a similar approach to that for electronic and radical stabilization descriptors, isodesmic reactions have also been proposed to describe steric effect. For example, the following reaction was studied by Rüchardt and Beckhaus:[31]

$$R-Ph_3 + CH_4 \rightleftharpoons R-H + H_3C-Ph_3 \quad (6)$$

This method proved unsuccessful due to intramolecule hydrogen transfer contamination from resonance effects. Recently, Böhm and Exner[73] proposed a similar approach to evaluate the steric effect by calculating the reaction energy of a different isodesmic reaction:
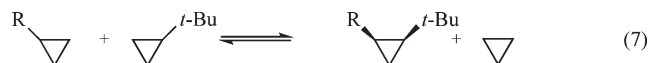
However, steric constants calculated via this method also differ distinctly from Charton steric parameters, particularly when we re-evaluated them for a subset of species in the present work using high level ab initio molecular orbital theory methods in place of density functional theory.

Spatial parameters offer a more direct approach to modeling the steric bulk of the system. In the field of organometallic chemistry, steric effects are often quantified through various molecular volume means. While molecular volume (V) can be very poor descriptor for steric effect, the Tolman's cone angle, θ, of the molecule (shown in Figure 3a) has been shown to be more successful.[3] Its value can be easily calculated using the van der Waals radius of the relevant atoms. Since the cone angle does not measure the overlap in molecules with congestion, the solid angle Ω was proposed.[56] Ω can be understood as the projection of the ligand onto a sphere at the origin of the bond-breaking site (see Figure 3b). For small molecules, the solid angle can be calculated easily, but for larger systems (such as those relevant to polymer or biological chemistry), this becomes computationally expensive, and the importance of congestion in describing steric effect is in any case arguable.[4] Since only the volume close to
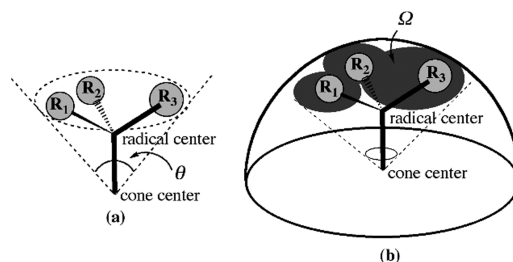

Figure 3. Tolman's cone angle and solid angle of an alkyl substituent.

the reaction center has an appreciable effect on the steric hindrance, anchor volume V^a and cone volume CV were also investigated as steric descriptors in the present work.

Other approaches to quantifying the steric effect of a substituent include the ligand repulsion energy E_R, as proposed by Brown.[5] This computes the steric effect for a substituent in a prototypical environment, and measures the size of the group within the context of its interactions with a specific molecular entity. It is based on the gradient of the van der Waals potential in relation to bond distance. In addition, we have also considered in this work the simplest possible steric quantifier, the order of the radical center. The radical *order* counts the number of non-hydrogen substituents bound to the radical center, giving methyl radical a value of zero, monosubstituted radicals one, secondary radicals two, and tertiary radicals three.

Literature values of the Charton steric descriptor (v), Dubois steric parameter (E'_s) and ligand repulsive energies (E_R), and computed values of molecular volume (V), anchor volume (V^a), cone volume (CV), Tolman's cone angle (θ), solid angle (Ω), and radical center *order* were used to determine the correlation between each of these parameters and the Charton steric descriptor (see Figure 4; raw data in Table S.2 of the Supporting Information). The correlation between E'_s and v is reasonably high ($R^2 = 0.66$) since these parameters are determined by similar methods. The correlation between E_R and v is quite high ($R^2 = 0.65$) as well, however E_R cannot be calculated easily. The various volume parameters offer a more direct approach to modeling the steric bulk of the alkyl radicals. The molecular volume V is a poor descriptor ($R^2 = 0.22$), as is the cone volume CV ($R^2 = 0.09$). The anchor volume, V^a shows only a slightly higher correlation with v than V ($R^2 = 0.30$).

As Tolman's cone angle θ was originally designed for use in inorganic chemistry, the distance between the radical center and cone center is normally specified as 2.28 Å, which is the typical metal ligand bond length. To estimate θ for our alkyl radicals, it is necessary to consider their geometries in compounds more relevant to chemical reactions under study. To this end, values of θ were calculated for the alkyl fragments R in corresponding series of optimized R−X compounds, for X = TEMPO, Br, Cl, and $SC(CH_3)=S$. In each case, the value θ obtained for a given R group was largely independent of X (see Table S.4 of the Supporting Information), indicating that any of these compounds might be used for generating the steric parameters. In this study, we selected θ computed from optimized R−Cl geometries, as providing the most computationally efficient access to Tolman's cone angles. The θ values calculated in this way show high correlation ($R^2 = 0.77$) with v. Although the solid angle Ω is designed to avoid interligand meshing, it shows low correlation ($R^2 = 0.36$) with v. It is likely that congestion is not a problem for these small alkyl radical groups and the direct cone angle therefore gives a better description of steric effect than the solid angle.
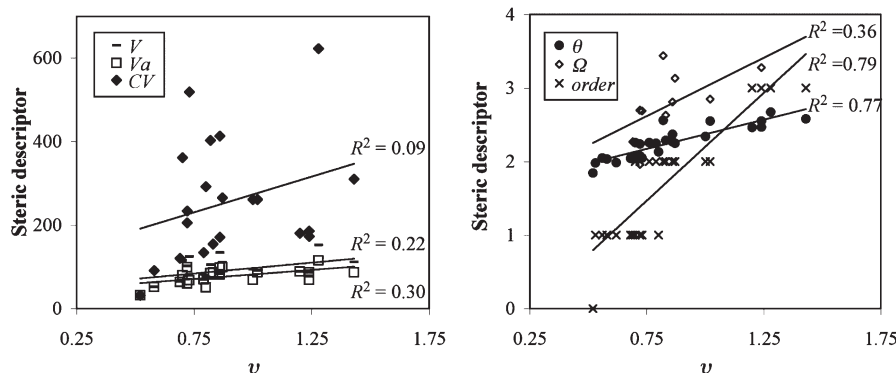
Figure 4. Comparison of the computed and empirical steric descriptors.

Finally, the radical order provides very simple way to measure steric effects. It shows a high degree of correlation ($R^2 = 0.79$) with v and is easily accessible since it requires no calculation, only the counting of non-hydrogen substituents around the radical center. However, from a chemical perspective, this does not appear to be a satisfactory way to measure steric effects. For example, it requires that groups such as t-Bu and cumyl ($^{\bullet}C(CH_3)_2Ph$) are described by the same descriptor. It is possible that its good correlation with other steric parameters may be caused by a very small variation in size of the second substituents in the training set (in our set, nearly all secondary radicals contain methyl groups and all tertiary radical contain two methyl groups). As a result we cannot rule out the possibility that the observed correlation may break down for larger tertiary radicals such as ($^{\bullet}CPh_3$). Given this risk, the other promising steric parameter studied, Tolman's cone angle θ, was selected for further consideration.

Radical Stability. Traditionally, radical stability is measured using the radical stabilization energy (RSE).[68] This is defined as the enthalpy change of the following reaction:

$$R^{\bullet} + CH_4 \rightleftharpoons R-H + {^{\bullet}CH_3} \qquad (8)$$
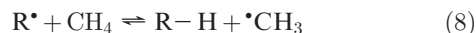
In essence, one compares the stabilities of $R^{\bullet}$ radical to a reference point, $^{\bullet}CH_3$, balancing the reaction with C−H bonds. In attributing substituent effects on RSEs to the differing stabilities of the radical species, one must implicitly assume that corresponding substituent effects on the C−H bonds of the closed shell species are negligible.[74] While this assumption is likely to be reasonable at a qualitative level for the C−H bonds in most carbon-centered radicals, it is an assumption and may potentially break down in some situations.

Alternative measures of relative radical stability have been also been proposed. In particular, the original linear free energy relationship for nitroxide combination reactions made use of Rüchardt[32] radical stabilization parameters (σ_{RS}). These are based on a semiempirical scheme in which radical stabilization energies of various $R^{\bullet}$ radicals are obtained from corrected R−R BDEs. The advantage of using R−R in place of R−H is that polar effects in the closed-shell compound are eliminated; the disadvantage is that corrections for steric strain in R−R (in this case obtained from MM2 force field calculations) are instead required. These RSE^{corr} values are then scaled according to the order of the radical center into primary, secondary and tertiary radicals and by the formation enthalpy of the methyl radical to give σ_{RS} values.[8] More recently, alternative schemes based on use of polar terms to correct various types of bond energies have also been developed.[75]

A more direct approach to measuring relative radical stability is through examination of the extent of delocalization of the unpaired electron in a radical; the more delocalized the unpaired electron, the more stabilized the radical is likely to be. Experimentally, this radical stabilization effect can be measured using electron spin resonance (ESR) data, where spin-coupling constants are correlated with the extent of electron delocalization (at least for planar radicals).[32,76] Spin density distributions can also be easily calculated directly by applying an electron localization scheme to the wave function obtained via a quantum-chemical calculation. This has the advantage of being applicable to both planar and nonplanar radicals. In this work, we examine the absolute value of Mulliken spin density[40] of the radical center, ρ; the higher the value of ρ, the more localized the radical and the less stabilized it is expected to be.

We also calculate the ratio of the spin density on the selected radical center to the sum of the absolute value of spin densities on the other non-hydrogen atoms in the molecule to give the delocalization of the spin density, $\rho\%$.[67] In doing this, we summed the contributions of hydrogen atoms into their corresponding non-hydrogen centers, as per standard practice.

$$\rho\% = \frac{|\rho(\text{nominal radical center})|}{\sum |\rho(\text{all other non-hydrogen centers})|} \qquad (9)$$

Iwao and co-workers have previously defined this as the ratio of spin density over carbon atoms only.[67] However, as some other heavy atoms can also bear large electron spin, the definition of the delocalization of the radical center above includes all other atoms.

Figure 5 shows the correlations between literature σ_{RS} values and Mulliken spin densities, ρ, delocalization of the spin density, $\rho\%$, and calculated RSEs; raw data are provided in Table S.3 of the Supporting Information. Values of the RSE were found to agree with the literature values published by Zipse,[77] calculated at the same level of theory. Correlation between ρ and σ_{RS} is very high ($R^2 = 0.91$), as is the correlation between RSE and σ_{RS} ($R^2 = 0.92$), while the correlation between the delocalization of the spin density, $\rho\%$, and σ_{RS} is not quite as high ($R^2 = 0.78$).

The high degree of correlation between the reaction-based parameters and spin densities provides confidence that the former are measuring the correct trends in radical stability for carbon centered radicals, and that either may be used in the linear free-energy relationship. We selected two descriptors for further study in the present work. The spin density ρ was chosen as the most direct measure of radical stability, independent of reaction energies. It also had the advantage that spin densities can be obtained accurately at relatively
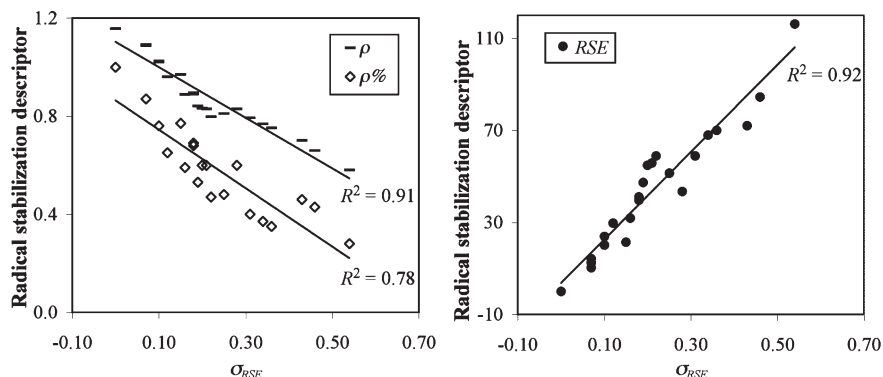
Figure 5. Comparison of the computed and empirical radical stabilization descriptors.

low levels of theory, making them more easily calculated for larger species. We also selected the traditional RSE as it is easily obtained from experimental bond dissociation energies, as well as theoretical calculation. The RSE, as a reaction-energy-based measure, does contain a contribution from the relative stabilities of $R^\bullet$ and $R-H$, which will be influenced by the steric cost associated the hybridization change from sp^2 to sp^3. The high correlation between RSE and spin is an indication that this steric effect is either relatively small or aliased with the same factors that affect the stabilization of the unpaired electron, but this effect may become important for certain bulkier radicals. Since this same steric effect is likely to be important in combination reactions of alkyl radicals with nitroxides, this may be an advantage for modeling these reaction energies. At the same time, the spin density is likely to provide the best parameter for establishing the relative importance of the various factors affecting the reaction energies.

Model for Variation of the Alkyl Radical with Fixed Nitroxide. On the basis of our examination of the available parameters we therefore selected two sets of descriptors for further study. The first set, which comprised μ, θ, and ρ, were chosen as the most direct measures of polar, steric and radical stabilization effects on alkyl radicals, and would be expected to be most useful in establishing the relative importance of these factors determining the reaction energies. The second set, which comprised RSE and IP, was chosen as the reaction energy based parameters that collectively measured the relative stabilities of $R^\bullet$ to the most important valence bond contributors of an alkoxyamine (i.e., $R^{+-}ONR'R''$ and $R-ONR'R''$, measured in the IP and RSE as the stabilities of R^+ and $R-H$ respectively). We now test each parameter set in turn by using them to model the reaction energies for the combination of a set of alkyl radicals with a fixed nitroxide, TEMPO (training set I).

Considering first the descriptors μ, θ, and ρ, we obtained the following model by fitting to our calculated 298 K gas-phase equilibrium constants for the combination reactions in training set I:

$$\log(K_{eq}) = -0.354\mu - 2.33\theta + 24.3\rho + 6.45 \qquad (10)$$

A plot of the fitted log (K_{eq}) values versus the corresponding *ab initio* data is provided in Figure 6; corresponding raw data is provided in Table S.5 of the Supporting Information. As is clear from this Figure, the model generally fits the data very well. However, the equation slightly underestimates K for **B1**, the only combination reaction with a methyl radical. This might be due to an overcompensation for steric effects in this system. It also substantially overestimates K for the
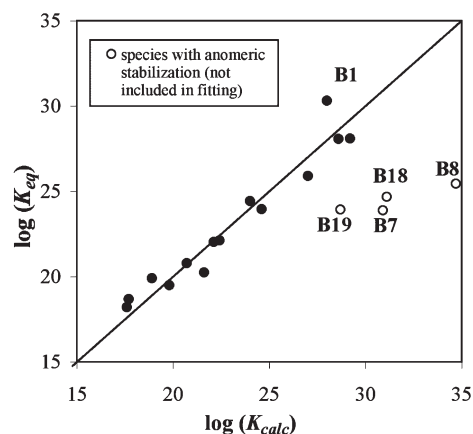

Figure 6. Comparison of directly calculated (K_{calc}) equilibrium constants with (K_{eq}) values fitted to μ, θ, and ρ for combination reactions of alkyl radicals with TEMPO at 298 K.

radical species $^\bullet CH_2OH$ (**7**), $^\bullet CH_2F$ (**8**), $^\bullet CH(CH_3)OC(O)-CH_3$ (**18**), and $^\bullet CH(CH_3)Cl$ (**19**). These latter radicals all possess a heteroatom in the position α to the radical center. Their higher reactivity is due to anomeric stabilization[78] of the product alkoxyamine species. This effect has been previously noted for TEMPO alkoxyamines derived from tetrahydrofuran and triethylamine,[79] and also for $-$SPh and acyl substituted TEMPO alkoxyamines,[22] all of which show higher energies of dissociation at the $C-O$ bond than expected. It has also been investigated using computational methods.[57] One of the lone pairs of the nitroxyl oxygen lies antiperiplanar to the carbon$-$heteroatom bond, allowing hyper-conjugation to occur between the lone pair and the σ^* antibonding orbital of the bond. This is illustrated in Figure 7 for the TEMPO$-CH_2OH$ alkoxyamine. In this example, anomeric stabilization results in a significant lengthening of the NOC(H$_2$)$-$OH bond while the NO$-CH_2OH$ bond is significantly shortened and strengthened.[57] It is therefore expected that in the absence of a descriptor quantifying anomeric stabilization the linear free-energy relationship will not accurately describe a combination reaction in which this effect is present in the product alkoxyamine species. Therefore, these systems were not included in the fitting. When these four points are excluded from the analysis, the model fits the remaining data extremely well, with an R^2 value of 0.94 and a mean absolute deviation just 4.4 kJ mol^{-1} in free energy.

However, despite the excellent fit of the equation to the data, it has some deficiencies as a model for these reactions. In particular, from the coefficients of μ, θ, and ρ, we note that the combination reaction is favored by an increase in ρ
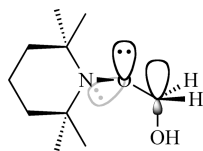
Figure 7. The alkoxyamine product of the reaction between TEMPO (B) and $^\bullet CH_2OH$, with anomeric stabilization of the NO–C bond.

(and hence a decrease in radical stability), and disfavored by increases in θ and μ (and hence an increase in polarity and steric bulk). Whereas the radical stability and steric effects are intuitive, the influence of polar effects is not. As explained above, given the polarity of the R-ONR′R″ bond, one would expect combination to be favored by *increases* to the polarity of R through increased resonance between R-ONR′R″ and R⁺⁻ONR′R″. In fact when the statistical significance of the various parameters was examined, neither the polar nor the steric descriptors were found to be significant at the 90% level of confidence. It is true that, for this limited data set, their significance did rise to 95% when the "outlier" **B1** was excluded from the fitting; but when the equation was later fitted to the most complete data set available (i.e., training sets I and II and the test set, with the anomeric outliers excluded) the significance of these terms was low, and the equation was therefore unsatisfactory.

The small role of polar and steric effects in the equation was also confirmed when we analyzed the relative contributions from each of the parameters using eqs 11 and 12,[80] previously used to analyze contributions to the dissociation rate coefficient.[8]

$$\alpha_X = \sqrt{\frac{\sum_{i=1}^{n}(X_i - \bar{X})^2}{\nu}} \tag{11}$$

$$\% X = 100 \times \frac{\alpha_X C_X}{\sum_j \alpha_{X_j} C_{X_j}} \tag{12}$$

Here X_i is the value of the parameter X for the ith data; $\bar{X}$ is the mean of the X parameter in n number of data points; ν is the degree of freedom, is defined as $n - 2$; α_X is the weighting coefficient and C_X the coefficient of the X parameter. From eqs 11 and 12, we calculated contributions from each descriptor in eq 10 to be 12%, 13%, and 75% for the polar, steric and radical stabilization energy, respectively.

Given the redundancy of the some of the parameters in eq 10, we then considered our reaction energy based parameters, RSE and IP. Equation 13 was obtained by fitting to Training Set I, but with the four anomerically stabilized species that were outliers in Figure 6 (i.e., **B7**, **B8**, **B18**, and **B19**) again omitted.

$$\log(K_{eq}) = -1.09\text{IP} - 0.199\text{RSE} + 39.8 \tag{13}$$

Figure 8 compares the fitted values, as obtained from eq 13, and the corresponding directly calculated values of the equilibrium constant, as obtained from our *ab initio* calculations; raw data is provided in Table S.6 of the Supporting Information. As is clear from this graph, the fit of the equation to the data is excellent, with an $R^2 = 0.94$ and MAD = 5.1 kJ mol⁻¹. The only significant outliers are the four anomerically stabilized species that were omitted from
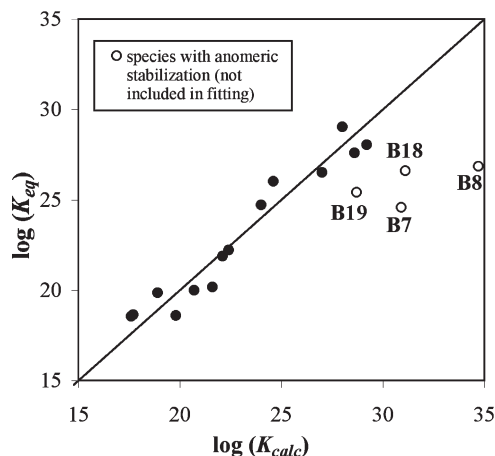

Figure 8. Comparison of directly calculated (K_{calc}) equilibrium constants with (K_{eq}) values fitted to IP and RSE for combination reactions of alkyl radicals with TEMPO at 298 K.

the fitting, all other points have deviations of 8.1 kJ mol⁻¹ or less.

From the coefficients of the parameters we find that combination is favored when the values of RSE and IP decrease, and hence as the relative stability of R• decreases and R⁺ increases. In other words, as expected, combination is favored by decreases to the stability of the reactant R•, and increases to the stability of the product alkoxyamine through increasing resonance with its ionic configuration R⁺⁻ONR′R″. On the basis of statistical testing, we find that both RSE and IP are significant at the 99% level of confidence, and have relative contributions of 78% and 22%, respectively. Once again, the stability of the alkyl radical is found to be the largest factor affecting the equilibrium constant of the combination reaction, though this term reflects to some extent the steric cost of the hybridization change from sp² to sp³ upon formation of an alkoxyamine. The increased importance of the polar term, IP, compared with eq 10 is probably partly due to the fact that, unlike the dipole moment, it also contains a contribution from the stability of the R• radical. Nonetheless, the fact that both RSE and IP are significant is a sign that polar effects are playing a role in this reaction, and that the IP is providing a better measure of these than the dipole moment. For this reason, the parameter set RSE and IP was chosen for modeling the effect of the chemical structure of the alkyl radical on the equilibrium constant for its combination reactions with nitroxides.

Descriptors for the Nitroxide Radical. To model the effect of the chemical structure of the nitroxide on the equilibrium constant for its combination reactions with alkyl radicals one might in principle consider adopting the same parameters designed for the alkyl radicals, though given the polarity of alkoxyamine bond the EA would be expected to provide a better measure of polar effects than IP in this case. However, during the course of our analysis we discovered that, for nitroxides, these terms are highly correlated with one another and essentially measure the same chemical properties. We therefore adopted just one of these parameters, the RSE, which we redefined using the following isodesmic reaction 14.

$$\text{RR}′\text{NO}^\bullet + (t\text{-Bu})_2\text{NOH} \rightleftharpoons \text{RR}′\text{NOH} + (t\text{-Bu})_2\text{NO}^\bullet \tag{14}$$

This is essentially the same as the standard RSE, reaction 8, but with the values systematically shifted to more
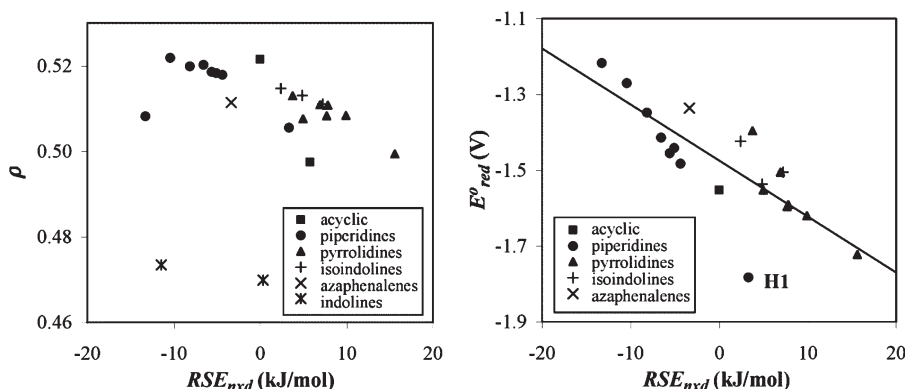
Figure 9. Comparison of RSE_{nxd} and (a) Mulliken spin density ρ on the nitroxide radical center ($R^2 = 0.007$) and (b) E^o_{red}($R^2 = 0.64$) of nitroxide radicals.

convenient sizes by using a nitroxide as the reference instead of $\cdot CH_3$. Reaction 14 is therefore referred to as the radical stabilization energy of a nitroxide radical, RSE_{nxd}. Although the computational expense of using dimethyl nitroxide as the reference species would be lower, the di-*tert*-butyl nitroxide species was selected in order to make RSE_{nxd} potentially more experimentally accessible.

Both reactions 8 and 14 contain contributions from the relative stabilities of the radical species and corresponding closed-shell species.[74] As shown above, for carbon centered radicals, the contribution of the closed shell species is minor and reaction 8 successfully models the relative stabilities of alkyl radicals, with trends following those expected from considering the substitution patterns on the radical, or the level of delocalization of the unpaired electron. For nitroxides, however, the contribution of the closed shell species is much more important, and Reaction 14 actually provides an excellent measure of the flexibility of the nitrogen center to pyramidalization upon formation of an alkoxyamine. To illustrate this, Figure 9, shows the relationship between RSE_{nxd} and the spin density on the nitroxide radical center, and between RSE_{nxd} and the calculated formal reduction potentials of the nitroxides in water, E^o_{red}, which we have previously determined.[51]

As seen in Figure 9a, the RSE_{nxd} values of the nitroxide radicals (shown in Scheme 1) do not correlate with the trend in spin densities, nor do they follow the trend expected based upon radical delocalization arguments. The most notable example is for the indoline nitroxides, which are expected to be more stable than the isoindoline nitroxides due to radical delocalization on the phenyl ring.[81] The indolines have much lower spin densities on the oxygen radical center than the isoindolines, indicating that radical delocalization occurs, however the RSE_{nxd} values do not reflect this stabilization.

By contrast, the correlation with the E^o_{red} values shown in Figure 9b is excellent, despite the fact that reaction 14 does not consider the ability of a nitroxide radical to accept an electron to form the corresponding anionic species. The reason for the excellent correlation is that both reduction and combination reactions lead to pyramidalization at nitrogen and, as we have discussed elsewhere,[51] the trends in reduction potentials are directly related to the flexibility of the ring structure of the nitroxide. At the same time, as in the case of the RSEs, the similarity of the reaction center and immediate chemical environment in all nitroxide radicals attenuates the influence of electronic substituent effects on the stability of the anions formed. The only significant outlier, **H1**, corresponds to the reaction of the only 2,2,6,6-tetraethyl-substituted TEMPO derivative in the training set;

it is possible that the additional steric effects of the ethyl groups on the combination reaction are not completely taken into account by the RSE_{nxd} parameter.

The parameter RSE_{nxd} therefore appears to provide a convenient measure of the ability of nitroxide radicals to form alkoxyamines, with increases to RSE_{nxd} reflecting decreases in the relative stabilities of an alkoxyamine due to lessening ease of pyramidalization at the nitrogen center. To explore this further, we fitted the following single parameter model to the methyl radical affinities of all the nitroxide radicals in training set II.

$$\log(K_{eq}) = -0.159 RSE_{nxd} + 27.3 \qquad (15)$$

Figure 10 shows the correlation between the logarithmic values of directly calculated equilibrium constants for combination reactions of methyl radical, $\log (K_{calc})$, and the corresponding fitted values; raw data is provided in Table S.7 of the Supporting Information. As it is clear from this figure, the fit of eq 15 to the data is very good ($R^2 = 0.90$), with an MAD equivalent to only 1.3 kJ mol^{-1} in free energy. As in the case of the reduction potentials, the largest 'outlier' corresponds to **H1**. In this case, the additional steric effects of the ethyl groups on the combination reaction are not completely taken into account by the RSE_{nxd} parameter, leading the fitted K to provide an upper bound to the true K value. Nonetheless, even here the magnitude of the deviation (6.7 kJ mol^{-1} in free energy) is relatively small. Although training set II only includes methyl radical affinities, we will show below that the equation also has good predictive value for reactions of larger substituted radicals with nitroxides, not included in the original training set. The use of the new nitroxide descriptor RSE_{nxd} provides an improvement upon previous descriptors,[9] which, although successful for most species, remained incomplete in the description of the steric effect for acyclic nitroxides.[82]

Linear Free-Energy Relationship. Having identified our descriptors, RSE, IP, and RSE_{nxd}, these were combined to form the following equation to describe $\log (K_{eq})$ for the combination reaction for various nitroxide radicals and common polymeric unimers.

$$\log(K_{eq}) = -1.16 IP - 0.184 RSE - 0.172 RSE_{nxd} + 38.9$$

$$(16)$$

The scaling factors of the parameters (expressed to three significant figures) were obtained by fitting the equation to the *ab initio* values of the equilibrium constant for the combination reaction for various nitroxide radicals and
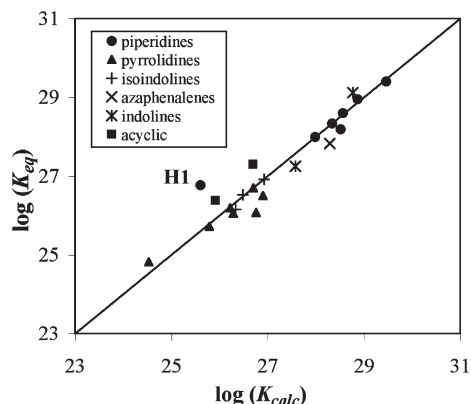
Figure 10. Comparison of directly calculated (K_{calc}) and fitted (K_{eq}) equilibrium constants for combination reactions of methyl radical with various nitroxides.
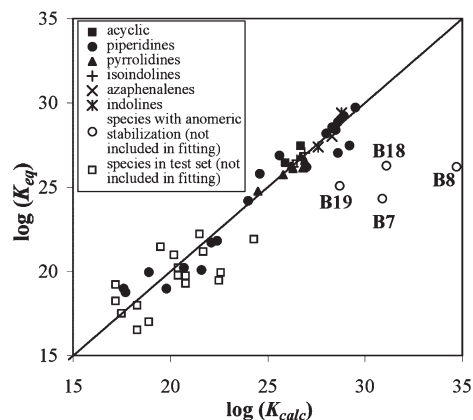

Figure 11. Comparison of directly calculated (K_{calc}) and fitted (K_{eq}) equilibrium constants for the full training and test sets of combination reactions.

common polymeric unimers making up training sets I and II. For the reasons detailed above, the four anomerically stabilized species were omitted from the fitting. The correlation between the fitted values, log (K_{eq}), and the directly calculated values, log (K_{calc}), is shown in Figure 11; corresponding raw data are provided in Table S.8 of the Supporting Information. The MAD between the K_{calc} and K_{eq} values is around half an order of magnitude, corresponding to 3.2 kJ mol^{-1} in free energy.

Although eq 16 was derived using only the fitting of methyl radicals with different nitroxides and larger alkyl radicals with TEMPO, its versatility can be shown through comparisons of some reasonably small mixed nitroxide and alkyl radical systems, for which direct calculation of the equilibrium constant is possible. The log (K_{calc}) and log (K_{eq}) values for combination reactions of the unimeric radicals of styrene (**13**), acrylic acid (**20**), methyl acrylate (**16**), acrylamide (**23**) and methyl methacrylate (**17**) by various nitroxide species (DBN (**A**), TEMPO (**B**), PROXYL (**I**) and TMIO (**P**)) have been added to Figure 11; corresponding raw data are provided in Table S.9 of the Supporting Information. The equation-calculated values show reasonably good correlation with the directly calculated values, with an MAD corresponding to 7.6 kJ mol^{-1} in free energy. It is observed that eq 15 performs well for the acrylic acid (**20**) and acrylamide (**23**) unimeric radicals, species not present in any of the reactions in the original training sets.

Having validated the equation by testing it on species not included in the fitting, it makes sense to refit the equation to all available data before carrying out more detailed analyses of the individual contributions from the various effects. To this end, we fitted the following equation to the combined training and test sets; omitting as before the four anomerically stabilized species.

$$\log(K_{eq}) = -1.10\text{IP} - 0.177\text{RSE} - 0.130\text{RSE}_{nxd} + 38.3$$

$$(17)$$

As expected, the fit of the equation to the data is good, with an $R^2 = 0.93$ and an MAD of 4.5 kJ mol^{-1} in free energy; all fitted values are provided in Table S.10 of the Supporting Information.

Examining the coefficients in the equation, we note that, as in our previous equations, combination is favored by decreases to IP (and hence an increase in stability of R$^+$), RSE (and hence a decrease in stability of R$^\bullet$) and RSE$_{nxd}$ (and hence an increase in the stability of the alkoxyamine). The relative contributions of the terms are 17%, 70%, and 13%,

respectively, though all are significant at the 99% level of confidence. It is therefore clear that the most important factor affecting the equilibrium constant for the combination reaction is stability of the alkyl radical. The smaller contributions of the other descriptors no doubt reflects the fact that all nitroxides have an identical reaction center up to at least the gamma position. In contrast to RSE of R$^\bullet$, which principally measures the stability of the isolated reactant radical, the other descriptors relate more strongly to the stability of the product alkoxyamine. The limited variation in chemical structure of the nitroxides in the vicinity of the formed bond therefore limits the influence of the other descriptors, both on the attacking alkyl radical and the nitroxide.

The fitted eq 17 can be used to determine gas-phase equilibrium constants of the control reaction of nitroxide-mediated polymerization for large systems where direct calculation is not feasible. However, it needs to be remembered that, in cases where anomeric stabilization of the alkoxyamine is possible (i.e., those having a lone pair donor group at the α-position), the predicted K may provide only a lower bound to its actual value. In its current form, eq 17 is parametrized for gas-phase equilibrium constants at 298 K and therefore does not give log (K) values directly comparable to experimental values performed in a solvent medium. It would be relatively straightforward to reparameterize the equation under any of the wide variety of experimental polymerization reaction conditions found in the literature. For the present, for simplicity, the standard state equation values are useful for comparison of the relative magnitudes of K, which are expected to follow the same trends in different temperatures and in common polymerization solvents.

Linear Free-Energy Relationship for Kinetics. Previous equations have described the combination and dissociation reaction rate constants, k_c and k_d, in terms of experimentally determined empirical descriptors.[7−9,63,83] In this work, a new equation was derived to describe the ratio of these two rate constants, $K = k_c/k_d$, in terms of computed descriptors. The individual rate constants can also be expressed in terms of the same parameters in order to demonstrate the use of the linear free-energy relationship in a more practical setting. The available experimental values of k_c, at 298 K in *tert*-butyl benzene (*t*BB),[7,63] and k_d, at 393 K and in *t*BB,[8,9,83] are shown in Table 4. These data sets were fitted using models based on the descriptors for alkyl radicals (IP, RSE) and nitroxide (RSE$_{nxd}$). The correlation between the fitted equation values and the experimental rate constants is shown for

Table 4. Experimental Rate Constants k_c (at 298 K in tBB) and k_d (at 393 K in tBB) for Combination Reactions of Alkyl Radicals with Nitroxides

species	log (k_c)	log (k_d)	IP (eV)	θ (deg)	RSE (kJ mol^{-1})	RSE$_{nxd}$ (kJ mol^{-1})
A12	8.3[a]	−3.7[d]	7.39	2.06	59.0	0.0
A13		−1.9[e]	7.03	2.37	68.0	0.0
B1		−11.2[f]	9.88	1.85	0.0	−4.3
B6		−5.0[f]	7.22	2.47	29.7	−4.3
B10		−3.5[f]	9.36	2.25	47.3	−4.3
B11		−0.9[f]	8.64	2.46	59.0	−4.3
B12	8.4[a]	−5.0[f]	7.39	2.06	59.0	−4.3
B13	8.3[a]	−3.3[f]	7.03	2.37	68.0	−4.3
B14	7.7[a]	−1.1[f]	6.73	2.67	69.9	−4.3
B15	9.4[a,b]	−7.1[f]	9.91	2.13	21.5	−4.3
B16		−4.5[f]	8.92	2.34	41.2	−4.3
B17	8.8[a,b]	−1.7[f]	8.27	2.58	54.9	−4.3
B25		−4.1[f]	8.27	2.27	72.0	−4.3
B26		−3.4[f]	7.64	2.04	84.6	−4.3
B28		3.8[f]	6.95	2.24	116.2	−4.3
B29		−7.6[f]	7.53	2.25	20.2	−4.3
I13		−3.8[e]	7.03	2.37	68.0	9.9
P13	8.2[c]	−4.2[e]	7.03	2.37	68.0	7.2
P14	8.1[a]	−2.4[d,g]	6.73	2.67	69.9	7.2
V4		−8.1[f]	8.21	2.05	10.3	5.8
V6		−4.2[f]	7.22	2.47	29.7	5.8
V9		−3.7[f]	10.31	2.04	31.9	5.8
V10		−2.6[f]	9.36	2.25	47.3	5.8
V11		0.1[h]	8.64	2.46	59.0	5.8
V12	7.0[a]	−3.5[f]	7.39	2.06	59.0	5.8
V13	6.5[a]	−2.3[f]	7.03	2.37	68.0	5.8
V14	5.3[a]	0.2[d]	6.73	2.67	69.9	5.8
V15	8.9[a,b]	−5.4[f]	9.91	2.13	21.5	5.8
V16		−2.5[f]	8.92	2.34	41.2	5.8
V17	6.4[a,b]	−0.1[h]	8.27	2.58	54.9	5.8
V20		−3.0[f]	9.2	2.29	41.2	5.8
V21		−2.7[f]	9.05	2.55	39.7	5.8
V22		−0.6[f]	8.5	2.55	55.8	5.8
V24		−2.4[f]	9.65	2.56	43.4	5.8
V25		−3.1[f]	8.27	2.04	72.0	5.8
V27		−2.9[f]	7.99	2.08	51.4	5.8
V29		−7.2[f]	7.53	2.25	20.2	5.8

[a] Reported by Sobek et al.[63] [b] Measured in acetonitrile. [c] Reported by Fischer et al.[7] [d] Reported by Marque et al.[21] [e] See Marque[9] and references within.[7] [f] Reported by Bertin et al.[8] [g] Determined from the estimated activation energy. [h] Reported by Beaudoin et al.[83]
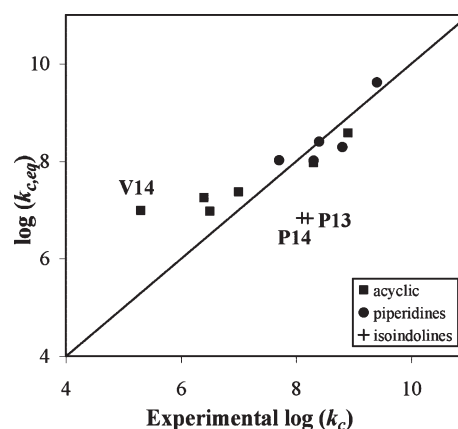
the combination rate constant, k_c, in Figure 12 and for the dissociation rate constant, k_d, in Figure 13; raw data are provided in Tables S.11 and S.12 of the Supporting Information. The equations obtained are shown below:

$$\log(k_{c,eq}) = -0.408\text{IP} - 0.0597\text{RSE} - 0.103\text{RSE}_{nxd} + 14.5 \tag{18}$$

$$\log(k_{d,eq}) = 0.554\text{IP} + 0.101\text{RSE} + 0.114\text{RSE}_{nxd} - 13.3 \tag{19}$$

For combination, the experimental and equation values show an MAD of just over half an order of magnitude. However, as the combination rates show little variation, all being close to 10^8 L mol^{-1}s^{-1}, the correlation seen in Figure 12 is poor ($R^2 = 0.51$). From the coefficients in the equation, we note that the combination rate becomes larger as IP, RSE and RSE$_{nxd}$ decrease. This indicates that is favored by decreases to IP (and hence an increase in stability of R$^+$), RSE (and hence a decrease in stability of R$^\bullet$) and RSE$_{nxd}$ (and an increase in the stability of the alkoxyamine). The relative contributions of the terms are 23%, 50%, and 27% respectively. However, based on a t test, only RSE$_{nxd}$ is significant at the 90% level of confidence, presumably due to the very limited variation in the combination rate data.

The largest deviations are seen for the isoindoline combination reactions **P13** and **P14**, and the SG1 combination

Figure 12. Correlation ($R^2 = 0.51$) between experimental combination rate constants and the fitted eq 18.

reaction **V14**. This may simply reflect the difficulty in measuring the experimental data for these very fast reactions; in that regard, it is worth remembering that the magnitudes of the deviations are themselves relatively small (ca. 1.5 orders of magnitude). Additionally, however, this may be due to the attenuating influence of diffusion effects on the combination rate coefficients. It has previously been argued that the combination reaction is not a diffusion-controlled process and has rate constants around an order of magnitude lower than those of the bimolecular self-reactions
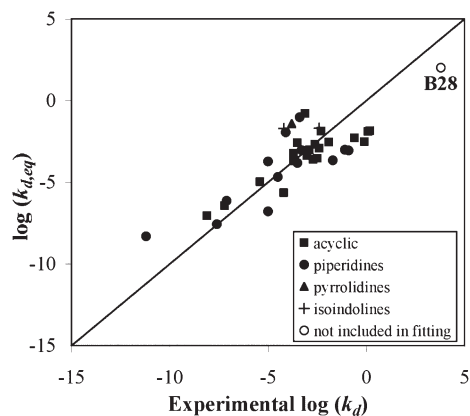
Figure 13. Correlation ($R^2 = 0.62$) between experimental dissociation rate constants and the fitted eq 19.

of the alkyl radicals.[84] This is shown by the spread in values for the experimental rate constants; a diffusion-controlled process would lead to a relatively constant value for the combination rate constants for a specific reaction medium and temperature. Nonetheless, as the rates of these reactions are close to the diffusion limit, varying degrees of attenuation of the rate coefficients due to diffusion effects might be anticipated, leading to scatter in the experimental data, and causing the equation fitting to be less successful than that for the equilibrium constant.

In contrast, values of the dissociation rate coefficient are much slower and are spread over a much larger range. However, these values also show only a poor fit by the equation for $\log(k_{d,eq})$, with an R^2 value of 0.62 and an MAD from experimental values of just over an order of magnitude in rate. The principal outlier, **B28**, is for the reaction of TEMPO with the cyclohexadienyl radical. In this case a competing side reaction (hydrogen abstraction from the cyclohexadienyl radical to form benzene) may be affecting the experimentally measured results, and therefore this species was not included in the fitting. As expected, the rate of dissociation becomes larger as IP, RSE, and RSE_{nxd} increase. The relative contributions of the terms are 18%, 64% and 18% respectively, and all are significant at the 95% level of confidence.

The poor fit seen for the dissociation rate constant may be due to extra steric effects not incorporated into the RSE descriptor. It is possible that the steric parameter is much more important in the description of the transition state of the reaction, but not in the reactants or products. With this in mind we performed a second fit with the addition of the term θ, which measures the steric effect of the alkyl radical. Equations 20 and 21 show the fittings of k_c and k_d to the data in Table 4; raw data are provided in Tables S.13 and S.14 of the Supporting Information.

$$\log(k_{c,eq}) = -0.0388\text{IP} - 0.737\theta - 0.0302\text{RSE}$$
$$-0.100\text{RSE}_{nxd} + 11.7 \qquad (20)$$

$$\log(k_{d,eq}) = 0.794\text{IP} + 5.68\theta + 0.0873\text{RSE}$$
$$+0.0821\text{RSE}_{nxd} - 27.7 \qquad (21)$$

The fitting to k_c in eq 20 does not show improvement over eq 18, with an R^2 value of 0.52 and an MAD from experimental values of just over half an order of magnitude in rate. According to the equation, the rate of combination becomes larger as IP, θ, RSE, and RSE_{nxd} decrease, consistent with

expectations. As before, only RSE_{nxd} is statistically significant in the k_c equation at the 90% level of confidence, though this is presumably due (at least in part) to the limited variation in the data. The relative contributions of the terms IP, θ, RSE, and RSE_{nxd} are 3%, 15%, 40%, and 42% respectively, indicating that radical stability is also likely to be playing a role.

In contrast to k_c, the fitting to k_d in eq 21 shows a marked improvement over the fitting in eq 19. In this case the R^2 value of the fitting is 0.83 and the MAD is less than an order of magnitude from the experimental data. As expected, the rate of dissociation increases as IP, θ, RSE, and RSE_{nxd} increase with all descriptors showing significance at the 95% level of confidence. The relative contributions of the terms IP, θ, RSE, and RSE_{nxd} are 20%, 29%, 42%, and 10% respectively. Comparison of the R^2 and MAD values for the fittings of k_d shown in eqs 19 and 21 confirm that the steric descriptor has a large effect on the fitting of the dissociation rate constant. Therefore, eq 21, including the extra steric descriptor θ is a better equation to describe k_d.

Conclusions

High-level *ab initio* molecular orbital theory calculations have been used to study the effects of substituents on the combination reactions of alkyl radicals with nitroxide radicals, with a view to developing general and convenient models for predicting the kinetics and thermodynamics of this process in terms of the molecular properties of each of the radicals. On the basis of our analysis, we selected the ionization potential (IP) and radical stabilization energy (RSE) of the alkyl radicals, a modified radical stabilization energy (RSE_{nxd}) as the nitroxide descriptor. We show that the alkyl radical descriptors model the relative stabilities of the alkyl fragment in the reactants (i.e., as R•) and product (i.e., as R−ONR′R″), the latter through consideration of the stability of R in the two principal valence bond configurations, R−ONR′R″ and R^{+-}ONR′R″. The nitroxide radical descriptor, though formally a radical stabilization energy, effectively measures the flexibility of the nitroxide radical to pyramidalization at nitrogen upon formation of the alkoxyamine. All three parameters are easily accessible through ab initio calculations or experiment. Using our descriptors, the following equation was obtained from a fit to a large set of calculated gas-phase equilibrium constants for the combination reaction: $\log(K_{eq}) = -0.10\text{IP} - 0.177\text{RSE} - 0.130\text{RSE}_{nxd} + 38.3$. The fit to the data was excellent, except in the small number of cases where anomeric effects are present; in those cases the equation provides a lower bound to the true result. The equation also had excellent predictive power when used to predict the behavior of reactions not included in the initial training sets. Variants of the equation were also successfully fitted to available experimental data for k_c, at 298 K and k_d, at 393 K, both in *tert*-butyl benzene; however, the inclusion of an additional parameter θ was necessary for the fitting of k_d due to additional steric effects present in the transition state of the reaction. On the basis of our analysis, it appears that the most important factor affecting the kinetics and thermodynamics of the combination reaction is the stability of the attacking alkyl radical, with smaller but significant contributions from the other parameters in the model. The multiparameter analysis completed in this work shows scope for being generalized to the study of other controlled radical polymerization reactions such as atom transfer radical polymerization (ATRP) and reversible addition−fragmentation chain transfer (RAFT), and work is currently underway to compare the roles of polar, steric, stabilization effects in these other reactions.

As part of this work, we also calculated solution-phase equilibrium constants for the reactions for which experimental

Hodgson et al.

data are available for benchmarking purposes. Our calculations reproduced the experimental results to within chemical accuracy, further highlighting the value of quantum chemistry as a predictive tool in this field.

Supporting Information Available: Tables S.1−S.14, showing calculated and fitted data, as well as Appendix S1, showing the B3-LYP/6-31G(d) optimized geometries in the form of GAUSSIAN archive entries. This material is available free of charge via the Internet at http://pubs.acs.org.

References and Notes

(1) (a) Taft, R. W. *J. Am. Chem. Soc.* **1953**, *75*, 4538. (b) Taft, R. W. *J. Am. Chem. Soc.* **1953**, *75*, 4534. (c) Taft, R. W. *J. Am. Chem. Soc.* **1952**, *74*, 3120. (d) Taft, R. W. *J. Am. Chem. Soc.* **1952**, *74*, 2729.
(2) (a) Mayr, H.; Patz, M. *Angew. Chem., Int. Ed. Engl.* **1994**, *33*, 938. (b) Mayr, H.; Kempf, B.; Ofial, A. R. *Acc. Chem. Res.* **2003**, *36*, 66. (c) Mayr, H.; Bug, T.; Gotta, M. F.; Hering, N.; Irrgang, B.; Janker, B.; Kempf, B.; Loos, R.; Ofial, A. R.; Remennikov, G.; Schimmel, H. *J. Am. Chem. Soc.* **2001**, *123*, 9500.
(3) Tolman, C. A. *Chem. Rev.* **1977**, *77*, 313.
(4) Immirzi, A.; Musco, A. *Inorg. Chim. Acta* **1977**, *25*, L41.
(5) Brown, T. L. *Inorg. Chem.* **1992**, *31*, 1286.
(6) (a) Dove, S.; Franke, R. *QSAR Comb. Sci.* **1991**, *10*, 23. (b) Dove, S.; Franke, R. *QSAR Comb. Sci.* **1991**, *10*, 16.
(7) Fischer, H.; Marque, S. R. A.; Nesvadba, P. *Helv. Chim. Acta* **2006**, *89*, 2330.
(8) Bertin, D.; Gigmes, D.; Marque, S. R. A.; Tordo, P. *Macromolecules* **2005**, *38*, 2638.
(9) Marque, S. R. A. *J. Org. Chem.* **2003**, *68*, 7582.
(10) Solomon, D. H.; Rizzardo, E.; Cacioli, P. U.S. Patent 4,581,429, March 27, **1985**.
(11) Rizzardo, E. *Chem. Aust.* **1987**, *54*, 32.
(12) Georges, M. K.; Veregin, R. P. N.; Kazmaier, P. M.; Hamer, G. K. *Macromolecules* **1993**, *26*, 2987.
(13) (a) Kato, M.; Kamigaito, M.; Sawamoto, M.; Higashamura, T. *Macromolecules* **1995**, *28*, 1721. (b) Wang, J.-S.; Matyjaszewski, K. *Macromolecules* **1995**, *28*, 7901. (c) Wang, J.-S.; Matyjaszewski, K. *J. Am. Chem. Soc.* **1995**, *117*, 5614.
(14) Chiefari, J.; Chong, Y. K.; Ercole, F.; Krstina, J.; Jeffery, J.; Le, T. P. T.; Mayadunne, R. T. A.; Meijs, G. F.; Moad, C. L.; Moad, G.; Rizzardo, E.; Thang, S. H. *Macromolecules* **1998**, *31*, 5559.
(15) Fukuda, T.; Terauchi, T.; Goto, A.; Ohno, K.; Tsujii, Y.; Miyamoto, T.; Kobatake, S.; Yamada, B. *Macromolecules* **1996**, *29*, 6393.
(16) Skene, W. G.; Belt, S. T.; Connolly, T. J.; Hahn, P.; Scaiano, J. C. *Macromolecules* **1998**, *31*, 9103.
(17) Bacon, C. A.; Cameron, N. R.; Reid, A. J. *Macromol. Chem. Phys.* **2003**, *204*, 1923.
(18) (a) Fischer, H. *Macromolecules* **1997**, *303*, 5666. (b) Fischer, H. *J. Polym. Sci., Part A: Polym. Chem.* **1999**, *37*, 1885. (c) Fischer, H.; Souaille, M. *Chimia* **2001**, *55*, 109.
(19) (a) Souaille, M.; Fischer, H. *Macromolecules* **2000**, *33*, 7378. (b) Souaille, M.; Fischer, H. *Macromolecules* **2001**, *34*, 2830. (c) Souaille, M.; Fischer, H. *Macromolecules* **2002**, *35*, 248. (d) Souaille, M.; Fischer, H. *Macromol. Symp.* **2001**, *174*, 231.
(20) Ananchenko, G. S.; Fischer, H. *J. Polym. Sci., Part A: Polym. Chem.* **2001**, *39*, 3604.
(21) Marque, S. R. A.; Le Mercier, C.; Tordo, P.; Fischer, H. *Macromolecules* **2000**, *33*, 4402.
(22) Marque, S. R. A.; Fischer, H.; Baier, E.; Studer, A. *J. Org. Chem.* **2001**, *66*, 1146.
(23) Schulte, T.; Studer, A. *Macromolecules* **2003**, *36*, 3078.
(24) Moad, G.; Rizzardo, E. *Macromolecules* **1995**, *28*, 8722.
(25) Fischer, H.; Kramer, A.; Marque, S. R. A.; Nesvadba, P. *Macromolecules* **2005**, *38*, 9974.
(26) Hansch, C.; Leo, A.; Taft, R. W. *Chem. Rev.* **1991**, *91*, 165.
(27) Taft, R. W. *Steric Effects in Organic Chemistry*; Newman, M. S., Ed.; Wiley: New York, 1956; Chapter 13.
(28) Gallo, R. *Prog. Phys. Org. Chem.* **1983**, *14*, 115.
(29) Fujita, T.; Iwamura, H. *Top. Curr. Chem.* **1983**, *114*, 119.
(30) Charton, M. *Top. Curr. Chem.* **1983**, *114*, 57.
(31) Rüchardt, C.; Beckhaus, H.-D. *Top. Curr. Chem.* **1985**, *130*, 1.
(32) Brocks, J. J.; Beckhaus, H. D.; Beckwith, A. L. J.; Rüchardt, C. *J. Org. Chem.* **1998**, *63*, 1935.
(33) Fujita, T.; Takayama, C.; Nakajima, M. *J. Org. Chem.* **1973**, *38*, 1623.
(34) Lien, E. J. In *Advances in Quantitative Structure-Property Relationships*; Charton, M., Ed.; Jai Press Inc.: Greenwich CT, 1996; Vol. *1*, pp 171−219.
(35) Guillaneuf, Y.; Gigmes, D.; Marque, S. R. A.; Tordo, P.; Bertin, D. *Macromol. Chem. Phys.* **2006**, *207*, 1278.
(36) Bertin, D.; Dufils, P.-E.; Durand, I.; Gigmes, D.; Giovanetti, B.; Guillaneuf, Y.; Marque, S. R. A.; Phan, T.; Tordo, P. *Macromol. Chem. Phys.* **2008**, *209*, 220.
(37) Coote, M. L.; Davis, T. P. *Prog. Polym. Sci.* **1999**, *24*, 1217.
(38) Lin, C. Y.; Coote, M. L.; Petit, A.; Richard, P.; Poli, R.; Matyjaszewski, K. *Macromolecules* **2007**, *40*, 5985.
(39) Izgorodina, E. I.; Coote, M. L. *Macromol. Theory Simul.* **2006**, *15*, 394.
(40) Hehre, W. J.; Radom, L.; Schleyer, P. V. R.; Pople, J. A. *Ab Initio Molecular Orbital Theory*; Wiley: New York, 1986.
(41) Koch, W.; Holthausen, M. C. *A Chemist's Guide to Density Functional Theory*; Wiley-VCH: Weinheim, Germany, 2000.
(42) Frisch, M. J.; Trucks, G. W.; Schlegel, H. B.; Scuseria, G. E.; Robb, M. A.; Cheeseman, J. A., Jr.; Vreven, T.; Kudin, K. N.; Burant, J. C.; Millam, J. M.; Iyengar, S. S.; Tomasi, J.; Barone, V.; Mennucci, B.; Cossi, M.; Scalmani, G.; Rega, N.; Petersson, G. A.; Nakatsuji, H.; Hada, M.; Ehara, M.; Toyota, K.; Fukuda, R.; Hasegawa, J.; Ishida, M.; Nakajima, T.; Honda, Y.; Kitao, O.; Nakai, H.; Klene, M.; Li, X.; Knox, J. E.; Hratchian, H. P.; Cross, J. B.; Adamo, C.; Jaramillo, J.; Gomperts, R.; Stratmann, R. E.; Yazyev, O.; Austin, A. J.; Cammi, R.; Pomelli, C.; Ochterski, J. W.; Ayala, P. Y.; Morokuma, K.; Voth, G. A.; Salvador, P.; Dannenberg, J. J.; Zakrzewski, V. G.; Dapprich, S.; Daniels, A. D.; Strain, M. C.; Farkas, O.; Malick, D. K.; Rabuck, A. D.; Raghavachari, K.; Foresman, J. B.; Ortiz, J. V.; Cui, Q.; Baboul, A. G.; Clifford, S.; Cioslowski, J.; Stefanov, B. B.; Liu, G.; Liashenko, A.; Piskorz, P.; Komaromi, I.; Martin, R. L.; Fox, D. J.; Keith, T.; Al-Laham, M. A.; Peng, C. Y.; Nanayakkara, A.; Challacombe, M.; Gill, P. M. W.; Johnson, B.; Chen, W.; Wong, M. W.; Gonzalez, C.; Pople, J. A. *Gaussian 03, Revision B.03*; Gaussian, Inc.: Pittsburgh PA, 2003.
(43) Werner, H.-J.; Knowles, P. J.; Amos, R. D.; Bernhardsson, A.; Berning, A.; Celani, P.; Cooper, D. L.; Deegan, M. J. O.; Dobbyn, A. J.; Eckert, F.; Hampel, C.; Hetzer, G.; Korona, T.; Lindh, R.; Lloyd, A. W.; McNicholas, S. J.; Manby, F. R.; Meyer, W.; Mura, M. E.; Nicklass, A.; Palmieri, P.; Pitzer, R.; Rauhut, G.; Schütz, M.; Stoll, H.; Stone, A. J.; Tarroni, R.; Thorsteinsson, T. *MOLPRO 2000.6*; University of Birmingham: Birmingham, U.K., 1999.
(44) Scott, A. P.; Radom, L. *J. Phys. Chem.* **1996**, *100*, 16502.
(45) Henry, D. J.; Sullivan, M. B.; Radom, L. *J. Chem. Phys.* **2003**, *118*, 4849.
(46) Izgorodina, E. I.; Brittain, D. B. R.; Hodgson, J. L.; Krenske, E. H.; Lin, C. Y.; Namazian, M.; Coote, M. L. *J. Phys. Chem. A* **2007**, *111*, 10754.
(47) (a) Cancès, M. T.; Mennucci, B.; Tomasi, J. *J. Chem. Phys.* **1997**, *107*, 3032. (b) Cossi, M.; Barone, V.; Mennucci, B.; Tomasi, J. *Chem. Phys. Lett.* **1998**, *286*, 253. (c) Mennucci, B.; Tomasi, J. *J. Chem. Phys.* **1997**, *106*, 5151.
(48) Tang, W.; Kwak, Y.; Braunecker, W.; Tsarevsky, N. V.; Coote, M. L.; Matyjaszewski, K. *J. Am. Chem. Soc.* **2008**, *130*, 10702.
(49) Lin, C. Y.; Coote, M. L.; Gennaro, A.; Matyjaszewski, K. *J. Am. Chem. Soc.* **2008**, *130*, 12762.
(50) Lin, C. Y.; Coote, M. L. *Aust. J. Chem.* **2009**, *62*, 1479.
(51) Hodgson, J. L.; Namazian, M.; Bottle, S. E.; Coote, M. L. *J. Phys. Chem. A* **2007**, *111*, 13595.
(52) Blinco, J. P.; Hodgson, J. L.; Morrow, B. J.; Walker, J. R.; Will, G. D.; Coote, M. L.; Bottle, S. E. *J. Org. Chem.* **2008**, *73*, 6763.
(53) van der Waals radii were taken from Bondi, A. *J. Phys. Chem.* **1964**, *68*, 441, except the value for H, which was taken from Rowland, R. S.; Taylor, R. *J. Phys. Chem.* **1996**, *100*, 7384. Radii not available in either of these publications were assigned $R_{vdW} = 2.00$ Å.
(54) http://www.ccdc.cam.ac.uk/products/csd/radii/ (retrieved 14 August, 2009). See for example: Allen, F. H. *Acta Crystallogr.*

2002, *B58*, 380. Cambridge Structural Database (CSD) covalent radii (R_{cov}) are used to assign bonded connections in crystal structures. A bonded connection is established if the distance (d) between two elements A and B is in the range from $R_{cov}(A) + R_{cov}(B) - t$ to $R_{cov}(A) + R_{cov}(B) + t$, where the tolerance ($t$) is usually set to 0.4 Å. The R_{cov} values have been refined over the years to minimize the need for editorial changes for specific structures. Elements not yet available in the CSD were assigned $R_{cov} = 1.50$ Å.

(55) Meyer, A. Y. *J. Chem. Soc., Perkin Trans. 2* **1986**, 1567.

(56) (a) Taverner, B. C.; Smith, J. M.; White, D. P.; Coville, N. J. *S. Afr. J. Chem.* **1997**, *50*, 59. (b) Taverner, B. C. *Steric* **1996**.

(57) Gaudel-Siri, A.; Siri, D.; Tordo, P. *ChemPhysChem* **2006**, *7*, 430.

(58) Gigmes, D.; Gaudel-Siri, A.; Marque, S. R. A.; Bertin, D.; Tordo, P.; Astolfi, P.; Greci, L.; Rizzoli, C. *Helv. Chim. Acta* **2006**, *89*, 2312.

(59) Izgorodina, E. I.; Coote, M. L. *Chem. Phys.* **2006**, *324*, 96.

(60) Lin, C. Y.; Izgorodina, E. I.; Coote, M. L. *Macromolecules* **2010**, *43*, 553.

(61) Ah Toy, A.; Chaffey-Millar, H.; Davis, T. P.; Stenzel, M. H.; Izgorodina, E. I.; Coote, M. L.; Barner-Kowollik, C. *Chem. Commun.* **2006**, 835.

(62) Coote, M. L. *Macromol. Theory Simul.* **2009**, *18*, 388.

(63) Sobek, J.; Martschke, R.; Fischer, H. *J. Am. Chem. Soc.* **2001**, *123*, 2849.

(64) Charton, M. *Prog. Phys. Org. Chem.* **1981**, *13*, 119.

(65) Parr, R. G.; Von Szentpaly, L.; Liu, S. B. *J. Am. Chem. Soc.* **1999**, *121*, 1922.

(66) Dubois, J. E.; MacPhee, J. A.; Panaye, A. *Tetrahedron Lett.* **1978**, 4099.

(67) Iwao, K.; Sakakibara, K.; Hirota, M. *J. Comput. Chem.* **1998**, *19*, 215.

(68) Benson, S. W. *Thermochemical Kinetics. Methods for the Estimation of Thermochemical Data and Rate Parameters*; John Wiley & Sons: New York, 1976.

(69) Hammett, L. P. *J. Am. Chem. Soc.* **1937**, *59*, 96.

(70) Charton, M. *Stud. Org. Chem.* **1991**, *42*, 629.

(71) Bertin, D.; Gigmes, D.; Marque, S. R. A.; Milardo, S.; Peri, J.; Tordo, P. *Collect. Czech. Chem. Commun.* **2004**, *69*, 2223.

(72) Ananchenko, G.; Beaudoin, E.; Bertin, D.; Gigmes, D.; Lagarde, P.; Marque, S. R. A.; Revalor, E.; Tordo, P. *J. Phys. Org. Chem.* **2006**, *19*, 269.

(73) Böhm, S.; Exner, O. *Org. Biomol. Chem.* **2008**, *6*, 1092.

(74) Coote, M. L.; Dickerson, A. B. *Aust. J. Chem.* **2008**, *61*, 163.

(75) See, for example: (a) Matsunaga, N.; Rogers, D. W.; Zavitsas, A. A. *J. Org. Chem.* **2003**, *68*, 3158. (b) de Vleeschouwer, F.; Van Speybroeck, V.; Waroquier, M.; Geerlings, P.; de Proft, F. *J. Org. Chem.* **2008**, *73*, 9109.

(76) Afanas'Ev, I. B. *Int. J. Chem. Kinet.* **1975**, *7*, 857.

(77) Zipse, H. *Top. Curr. Chem.* **2006**, *263*, 163. In this published work the RSE values were calculated using the reverse isodesmic reaction and therefore show the opposite sign from those calculated in this work.

(78) (a) Gorenstein, D. G. *Chem. Rev.* **1987**, *87*, 1047. (b) Juaristi, E.; Cuevas, G. *Tetrahedron* **1992**, *48*, 5019.

(79) Ciriano, M. V.; Korth, H.-G.; van Scheppingen, W. B.; Mulder, P. *J. Am. Chem. Soc.* **1999**, *121*, 6375.

(80) Shorter, J. *Correlation Analysis of Organic Reactivity*; J. Wiley & Sons: New York, 1982; pp 73−126.

(81) Guillaneuf, Y.; Gigmes, D.; Marque, S. R. A.; Astolfi, P.; Greci, L.; Tordo, P.; Bertin, D. *Macromolecules* **2007**, *40*, 3108.

(82) Studer, A.; Harms, K.; Knoop, C.; Muller, C.; Schulte, T. *Macromolecules* **2004**, *37*, 27.

(83) Beaudoin, E.; Bertin, D.; Gigmes, D.; Marque, S. R. A.; Siri, D.; Tordo, P. *Eur. J. Org. Chem.* **2006**, 1755.

(84) Beckwith, A. L. J.; Bowry, V. W.; Ingold, K. U. *J. Am. Chem. Soc.* **1992**, *114*, 4983.